

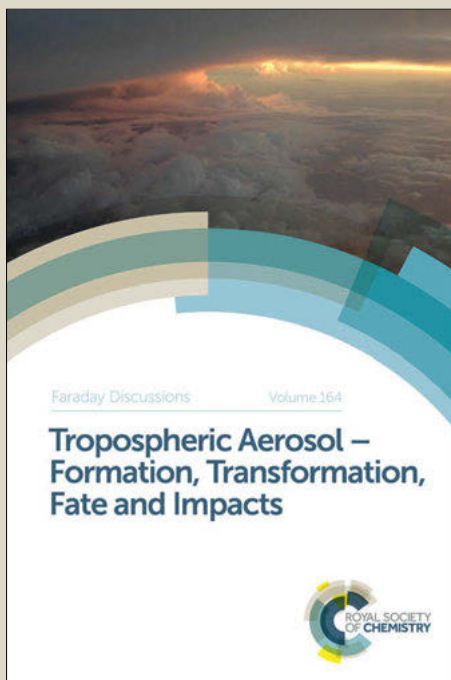
Faraday Discussions

Accepted Manuscript



This manuscript will be presented and discussed at a forthcoming Faraday Discussion meeting. All delegates can contribute to the discussion which will be included in the final volume.

Register now to attend! Full details of all upcoming meetings: <http://rsc.li/fd-upcoming-meetings>



This is an *Accepted Manuscript*, which has been through the Royal Society of Chemistry peer review process and has been accepted for publication.

Accepted Manuscripts are published online shortly after acceptance, before technical editing, formatting and proof reading. Using this free service, authors can make their results available to the community, in citable form, before we publish the edited article. We will replace this *Accepted Manuscript* with the edited and formatted *Advance Article* as soon as it is available.

You can find more information about *Accepted Manuscripts* in the [Information for Authors](#).

Please note that technical editing may introduce minor changes to the text and/or graphics, which may alter content. The journal's standard [Terms & Conditions](#) and the [Ethical guidelines](#) still apply. In no event shall the Royal Society of Chemistry be held responsible for any errors or omissions in this *Accepted Manuscript* or any consequences arising from the use of any information it contains.

Mechanochemical synthesis of Au, Pd, Ru and Re nanoparticles with lignin as a bio-based reducing agent and stabilizing matrix

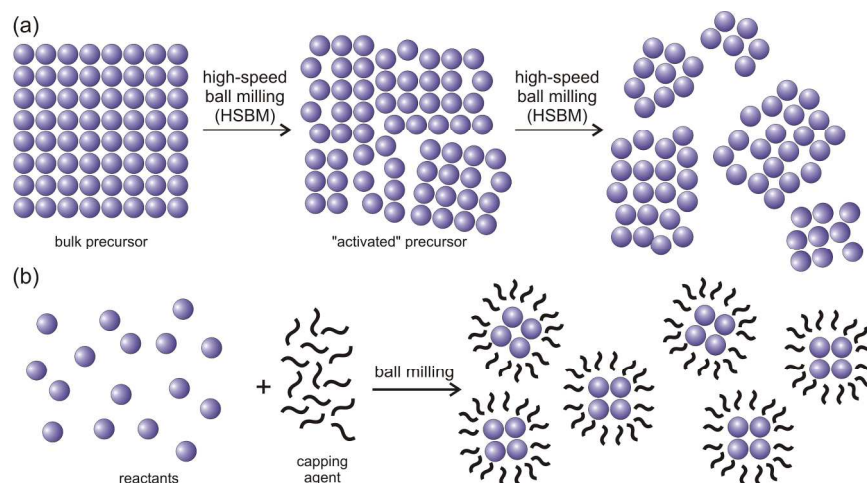
Monika J. Rak, Tomislav Friščić and Audrey Moores

5 DOI: 10.1039/b000000x [DO NOT ALTER/DELETE THIS TEXT]

A versatile, low-energy and solvent-free method to access nanoparticles (NPs) of four different transition metals, based on a bottom-up mechanochemical procedure involving milling of inorganic precursors, is presented. Lignin, a biomass waste, was effectively used as a reducing agent, for the first time in the mechanochemical context, to access MNPs where M=Au, Ru, Pd, Re. A series of metal precursors was used for this reaction and their nature was shown to be integral in determining whether NPs became incorporated within the organic lignin matrix, M@lignin, or not. Specifically, organometallic precursors resulted in extensive encapsulation of the NPs, as well as improved control over their size and shape, while ionic precursors afforded matrix-free NPs. The resulting NP-containing composites were characterized through Fourier-transform infrared attenuated total reflectance (FTIR-ATR) spectroscopy, transmission electron microscopy (TEM), X-ray photoelectron spectroscopy (XPS) and powder X-ray diffraction (PXRD). This mechanochemical grinding method for accessing M@lignin (M=Au, Ru, Pd and Re) is significantly more sustainable than the traditional solvent batch syntheses of metal NPs because it relies on the use of a biomass-based polymer, it is highly atom economical, it eliminates the need for solvents and it reduces drastically the energy input.

Introduction

25 Mechanical grinding or milling is one of the simplest and industrially highly relevant methods to obtain materials in the form of finely divided particles of micro- and nano-scale. This top-down approach to access nanoparticles (NPs) has been highly popular since 1960s and proceeds *via* comminution, *i.e.* mechanically crushing bulk material until a sufficiently small size is obtained (Scheme 1a).^{1, 2} Despite its simplicity, this approach relies on a significant input of mechanical energy to achieve the breakdown of hard inorganic materials and affords polydisperse NPs in a wide range of sizes and shapes and invariably leads to the appearance of surface defects and amorphization.^{3, 4} This surface deteriorating effect is the basis of mechanical activation of solids and has been recently studied extensively by the Šepelak group, who established the formation of 2-5 nm thick amorphous layers upon mechanical milling of oxide NPs.⁵ Recently, however, an alternative and innovative use of mechanical milling has been inaugurated for the synthesis of NPs, through a bottom-up process based on chemical reactions (Scheme 1b).^{6, 7}



Scheme 1. Illustrations of the (a) top-down comminuting and (b) bottom-up self-assembly approaches to the mechanochemical synthesis of NPs

This novel approach first centered on the synthesis of binary inorganic NPs and has largely been pioneered by the Baláz group, who conducted the simple metathesis reactions between soft metal salt solids (e.g. cadmium, zinc or lead chlorides and acetates) and soft solids acting as ionic or molecular sulfide sources (e.g. sodium sulfide, cystine etc) under solvent-free mechanochemical milling conditions.⁸⁻¹⁰ This method afforded monodisperse NPs of group II-VI metal chalcogenides. Such a bottom-up mechanochemical approach to NP synthesis is based on self-assembly processes, rather than particle comminuting. Specifically the nucleation of the new phase and the growth of nanocrystals occur in the presence of an effective capping agent that hinders NP agglomeration and prevents their growth beyond a certain size. The same principles were used by the group of Luque to synthesize ball-milled composites of magnetic iron oxide-based nanocatalysts into mesoporous structures and exploited them in catalysis.^{11, 12}

The self-assembly approach to NP synthesis is highly appealing as it proceeds under very low energy input, compared to both top-down mechanochemical and solvent-based self-assembly approaches.⁷ Moreover, the bottom-up mechanochemical approach ensures the formation of highly ordered structures with a high degree of monodispersity, in a similar fashion to solvent-based approaches which remain popular solutions to high-end applications. Mechanochemistry, however, has a much higher potential for scale-up than solvent-based techniques and can also drastically reduce waste generation.^{13, 14} In short, mechanochemical bottom-up synthesis of NPs has a strong potential to provide industry-compatible solutions, and their scope urgently needs to be widened to more materials.

Bottom-up mechanochemical synthesis of metal NPs

Besides for the synthesis of binary inorganic NPs, it was recently demonstrated that mechanochemical bottom-up assembly synthesis was also applicable to metal NPs. In this scheme, a metal salt is used as precursor and reduced during the mechanochemical synthesis. One of the first examples was the formation of AuNPs by reduction of potassium tetrachloroaurate(III) (KAuCl_4) with sodium borohydride (NaBH_4). The solvent-free reaction was conducted by mechanochemical milling

with poly(vinylpyrrolidone) as a protecting polymer, yielding AuNPs with sizes from 6 nm-28 nm diameter, depending on the ratio of components in the reaction mixture and milling time. This pioneering investigation of metal NPs synthesis through mechanochemical reduction was followed by a report of mechanochemical synthesis of gold-silver nanoclusters via a two-step process in which a chitosan biopolymer was used both as a protecting agent and a reducing agent in the presence of sodium hydroxide. Manual grinding of silver nitrate with chitosan using a mortar and pestle leads to the formation of AgNPs which galvanically reduce tetrachloroauric(III) acid (HAuCl₄) with further grinding and form NPs of a gold-silver alloy. Consequently, this work demonstrated the possibility of using galvanic reduction for the synthesis of metal NPs, as well as the use of a bio-based polymer, chitosan, both as a reducing and NP protecting agent.

We have recently demonstrated the mechanochemical synthesis of monodisperse AuNPs by mechanochemical galvanic reduction of HAuCl₄ in the presence of terminal monoalkylamines as capping agents. The reduction of HAuCl₄ was achieved without the need for external reductants by the action of the stainless steel milling assembly. The size of the resulting ultra-small AuNPs (diameter from 1 nm - 2 nm) was found to be readily controlled by the length of the alkyl chain on the capping agent, as well as by milling time.

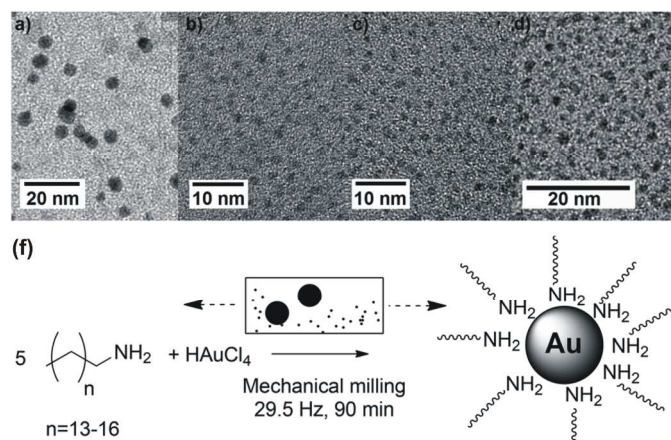


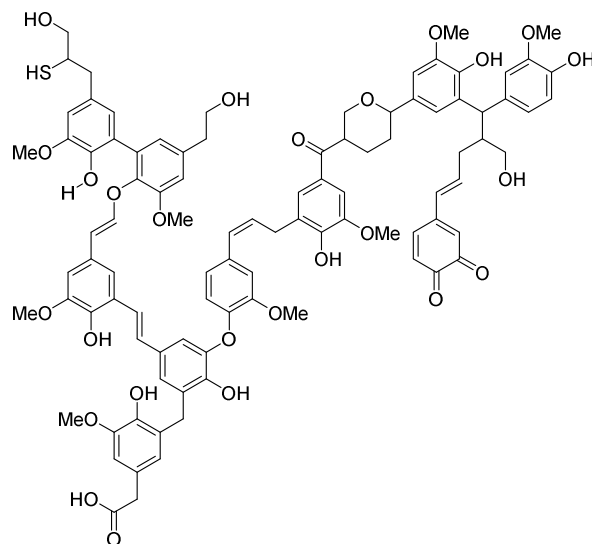
Figure 1. (a)-(e) Transmission electron microscopy (TEM) images of amine-protected AuNPs prepared by mechanochemical galvanic reduction of HAuCl₄ by stainless milling assembly and (f) schematic of the underlying reaction.⁷

Lignin as a mechanochemical reduction agent and matrix for NP dispersion

The current search for non-petroleum chemical feedstocks has focused much attention to biomass-derived polymers: lignin, cellulose, or hemicellulose.^{15, 16} The particular potential of lignin lies in a structure rich in aromatic residues with the potential to provide a source for a wide variety of aromatic compounds.¹⁷ The exploitation of lignin as an aromatic chemicals feedstock is hampered by the robustness of its extensive three-dimensional network structure, which renders this material intractably insoluble. However, it has been recently shown by Bolm's group that this polymeric structure can be broken down by mechanical grinding, milling or rubbing in the presence of a solid base, enabling subsequent dissolution.¹⁸ The mechanical degradation of biomass polymers is thought to proceed via radical

intermediates, as speculated in the early 1990's by Sumimoto *et al.* for the transformation of lignin into chromophores.^{19, 20} Mechanical breakdown of the lignin structure is thought to cause the formation of phenoxy radicals of considerable stability and, although the exact reaction is not fully understood, it is believed that the phenol groups adjacent to the methoxy groups in lignin structures can be oxidized and therefore used as reducing agents.

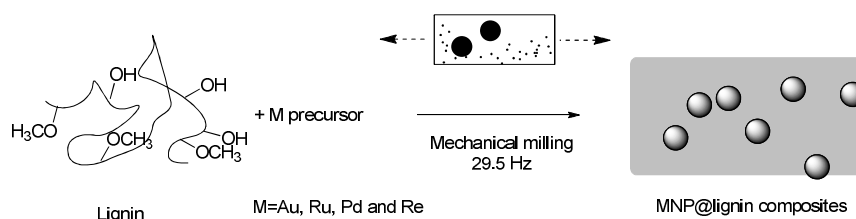
The increased interest in exploitation of biomass to form value-added products^{21, 22} has led to the synthesis of composite materials containing metal NPs and lignin (MNP@lignin). AuNPs@lignin was applied to Surface Enhanced Resonance Spectroscopy (SERS) detection of trinitrotoluene (TNT), as lignin could concentrate TNT in the vicinity of the AuNPs. In 2010, a proof of concept article by Lucas *et al.* showed that silver and gold NPs between 20 and 100nm may be incorporated in wood samples.²³ Pd and PtNPs@lignin were also produced and applied to catalytic oxidation and reduction reactions.²⁴ In these examples, the three-dimensional structure of lignin does not only provide reducing abilities for the generation of the composite, but also makes lignin a suitable solid support for NPs, allowing for easy separation of the catalyst through filtration.



Scheme 2. Proposed structure of Kraft pine lignin.²²

So far, most applications of lignin and lignin-based materials in NP technology have focused on its role as an abundant and inexpensive support material, and synthetic methods are based on conventional techniques. We now describe the first exploration of lignin as both a reduction agent and a NP dispersion matrix for the direct mechanochemical synthesis NP-lignin composites involving gold, palladium, ruthenium and rhenium (Scheme 3). In doing so, we also drastically expand the scope of existing mechanochemical synthesis of metal NPs, affording access to catalytically relevant materials. The reductive properties of lignin, that can be exploited in a solvent-free mechanochemical environment, have been utilized for *in situ* milling reduction of different metal precursors into NPs. Interestingly, the incorporation of the resulting NPs within lignin appears to be dependent on the nature of the metal precursor and its ability to mix readily with lignin. The produced

NP-lignin composites were characterized through transmission electron microscopy (TEM), X-ray photoelectron spectroscopy (XPS), powder X-ray diffraction (PXRD), and Fourier-transform infrared attenuated total reflectance spectroscopy (FTIR-ATR).



5

Scheme 3. Mechanochemical synthesis of MNP@lignin composites with M=Au, Pd, Ru and Re.

Experimental

Materials and Reagents

All chemicals and solvents were purchased from commercial sources and used without purification. Hydrogen tetrachloroaurate(III) hydrate, hexakis[μ -(acetato-O⁻)]-triqua- μ_3 -oxotriruthenium(III) (referred to as ‘basic Ru(III) acetate’ thereafter), palladium(II) acetate, palladium(II) acetylacetonate, and rhenium pentacarbonyl bromide were purchased from Strem Chemicals, Inc., ruthenium(III) chloride hydrate and palladium(II) chloride were purchased from Pressure Chemical. A Westvaco Chemical Division, Indulin AT Kraft pine lignin was purchased and used without further purification. This is a 99% lignin content free flowing brown powder lignin. 400-mesh carbon supported TEM grids were obtained from Electron Microscopy Science.

Equipment

High-resolution TEM and EDAX were performed using a Philips CM200 200 kV TEM. XPS was performed on a VG ESCALAB 3 MKII spectrometer (VG, Thermo Electron Corporation, UK) equipped with an Mg K α source. PXRD was performed using the Bruker D2 Phaser diffractometer using as CuK α source. A Retsch Mixer Mill MM 400 was used to perform milling experiments. A Perkin Elmer Spectrum Two FTIR with a single bounce diamond ATR was used for all FTIR measurements.

Typical procedure (synthesis of AuNP@lignin)

In a typical reaction a 10mL stainless steel milling jar was filled with a total of 200 mg of solid reagent material, consisting of 0.1 mmol of the metal precursor with the remainder being Kraft Lignin powder. To this reaction mixture were added two stainless balls of 7 mm diameter (1.34 grams weight, total ball-to-sample weight ~13). The jar was then closed and loaded onto the Retsch MM400 mixer mill. The reactions were conducted over 90 minutes, milling at a frequency of 29.5 Hz. At the end of the reaction, the solid product was scrapped out of the jar with a spatula and weighed. The product was placed onto a Kimwipe® filter plug in a Pasteur pipette and the solid washed using three 1 mL aliquots of water, followed by three 1 mL aliquots of acetone. The solid was allowed to dry under vacuum overnight and analyses were run on the dried samples. TEM grids were prepared by suspending the powders in acetone and depositing the resulting suspensions onto a 400-mess carbon

supported copper TEM grid. XPS samples were run by supporting dry samples onto carbon tape. The FTIR-ATR and PXRD measurements samples were conducted on solid dry samples.

5 Results

Mechanochemical milling of precursors of Au, Pd, Ru and Re with lignin was performed to establish the possibility to form the corresponding MNPs@lignin whereby NPs are embedded inside the lignin matrix to allow future applications. A summary of the results obtained is provided in Table 1.

10 Table 1. Summary of the results obtained by TEM and XPS after the mechanochemical reduction of metal precursors by lignin.

Metal precursor	Size (standard deviation)/nm ^a	Morphology of composite	Oxidation state (XPS)
HAuCl ₄	14.8 (6.8)	AuNPs in lignin	Au(0)
PdCl ₂	3.2 (1.6)	NPs outside of lignin ^b	Pd(0) and PdO
Pd(acetate) ₂	2.8 (0.7)	PdNP in lignin	Pd(0) and PdO
Pd(acetylacetonate) ₂	3.6 (0.9)	PdNP in lignin	Pd(0) and PdO
basic Ru(III) acetate	3.1(1.5)	RuNP in lignin	RuO
RuCl ₃	6.7 (4.2)	NPs outside of lignin ^c	RuO
Re(CO) ₅ Br	6.2 (1.5)	Snail eye morphology	ReO ₂

^a Based on TEM measurement

^b PdNPs were observed on the TEM grids of washed, solid phase product, outside of lignin

^c No RuNPs were observed with washed, solid phase product. RuNPs were visible on TEM grids
15 produced with the washings of reaction product

Preparation of AuNP@lignin composites

Mechanochemical milling of HAuCl₄ with Kraft lignin produced a dark purple loose powder. Characterization of the milled sample with TEM revealed the formation of a composite material in which high contrast metal-containing NPs were dispersed
20 throughout a low contrast matrix presumed to be lignin. Importantly, TEM analysis clearly demonstrated that the NPs are uniformly distributed throughout the volume of lignin (Figure 2a,b).

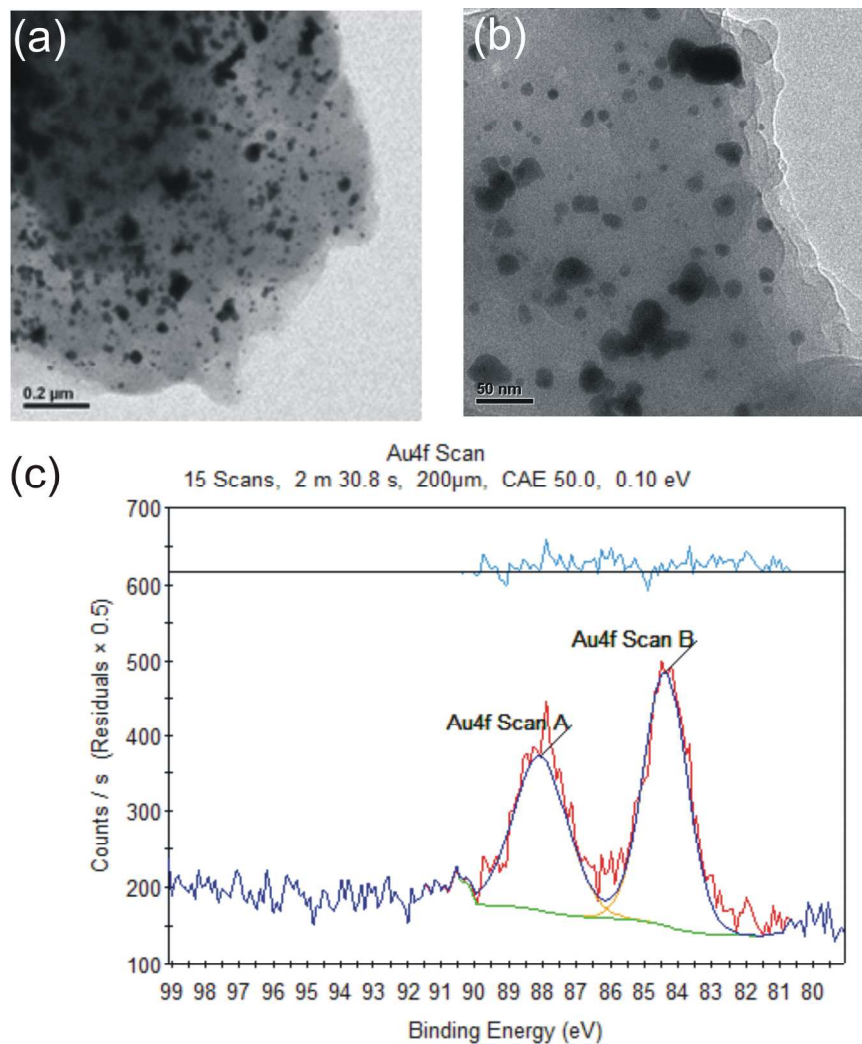


Figure 2. (a)-(b) Transmission electron microscopy (TEM) images of the mechanochemically prepared AuNP@lignin composite at different magnifications. (c) X-ray photoelectron spectrum of the AuNP@lignin composite.

5 The chemical composition of the NPs was established by X-ray photoelectron spectroscopy (XPS) which revealed the 4f signals characteristic for Au(0),²⁵ therefore confirming that the NPs are metallic gold (Figure 2c). The formation of AuNPs was also confirmed by powder X-ray diffraction (PXRD) analysis which revealed strong X-ray reflections consistent with (111), (200), (220), and (311)
10 reflections of metallic gold (Figure 3a).²⁶

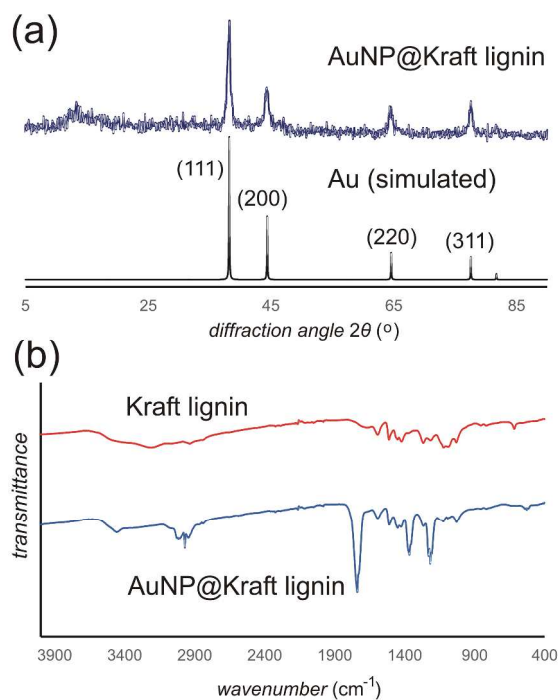


Figure 3. (a) Overlay of powder X-ray diffraction pattern of the prepared AuNP@lignin composite (top) and the one simulated for gold metal (bottom). (b) Overlay of FTIR-ATR spectra of precursor Kraft lignin (top) and a mixture of H₂AuCl₄ and Kraft lignin after milling for 90 minutes, corresponding to the AuNP@Kraft lignin composite.

The AuNPs embedded in the lignin matrix have an average diameter of 14.8 ± 6.8 nm and are larger than the ones we produced using amines.²⁴ This size is consistent with the Scherrer particle size analysis based on the PXR (Figure 3a) pattern, which gives a size of $14.3 (+/-2.1)$ nm (assuming a spherical particle shape). In all other herein explored samples the metal NPs were of considerably smaller sizes and were, consequently, difficult to identify by PXR which were generally dominated by a strong background generated by the amorphous lignin support (see ESI). In this reaction, we predicted that lignin would play the role of a reducing agent to afford Au(0) species. In order to verify this hypothesis, FTIR-ATR was used to detect oxidation of the lignin matrix. Whereas the FTIR-ATR spectrum of the Kraft lignin is dominated by extensive phenolic O-H stretching bands distributed around 3200 cm^{-1} , the spectra of AuNP@lignin were characterized by a strong C=O absorption band around 1700 cm^{-1} resulting from lignin oxidation (Figure 3b).

20 Preparation of PdNP@lignin composites

Next, we explored the possibility of mechanochemically synthesising lignin composites containing Pd NPs. Palladium(II) chloride (PdCl₂), palladium(II) acetate and palladium(II) acetylacetonate were selected as metal precursors for this experiment. Analysis by TEM revealed a significant difference in the morphology of the materials obtained with PdCl₂ vs the other two precursors (Figure 4).

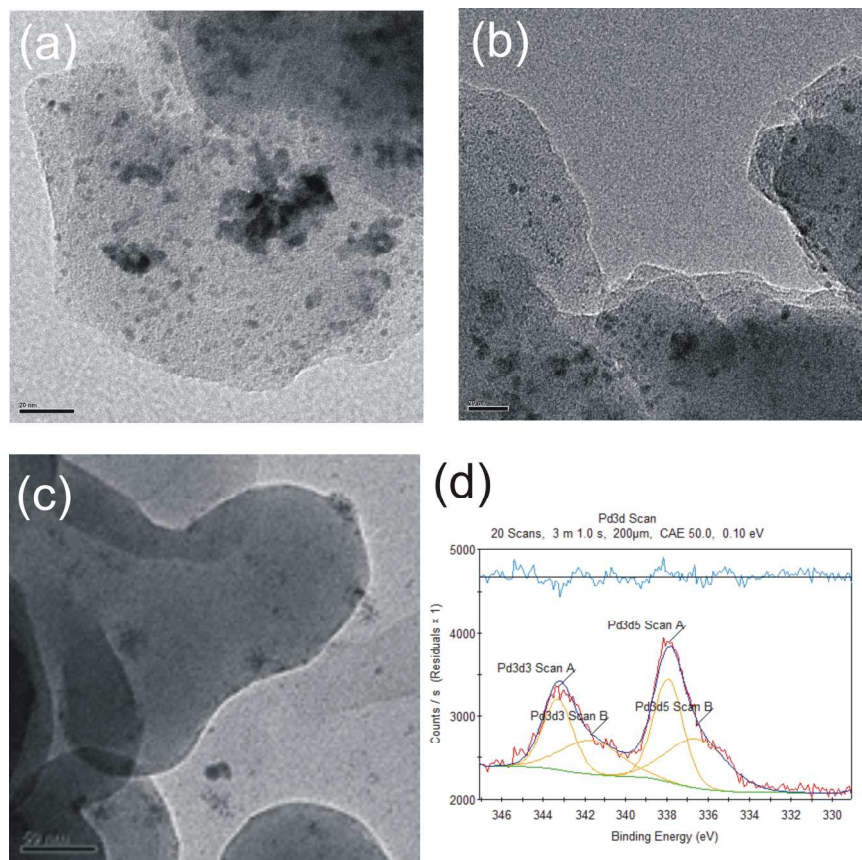


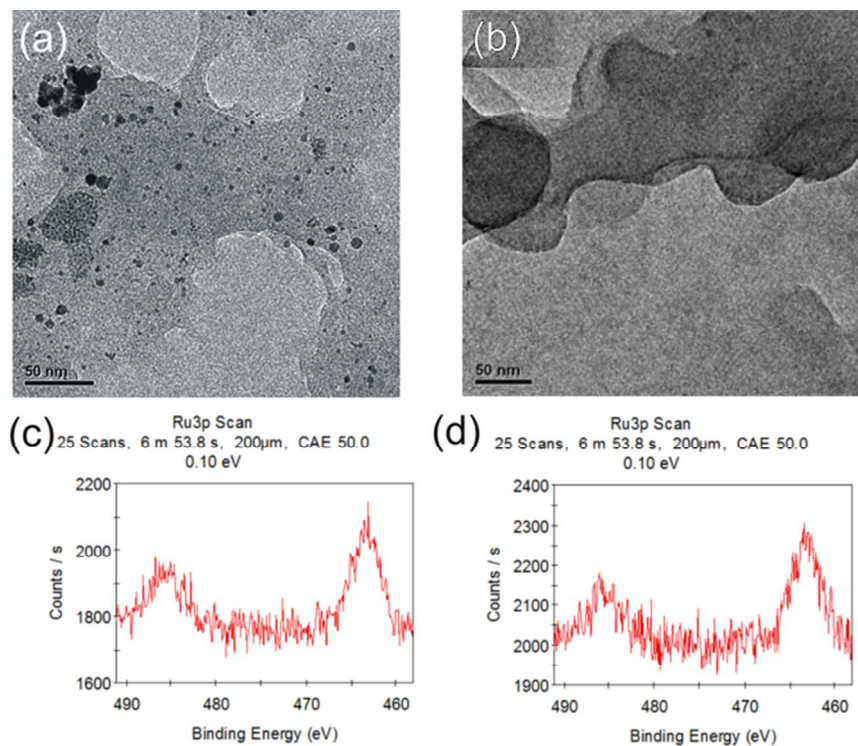
Figure 4. TEM images of samples prepared by mechanochemical reaction of Kraft lignin with: (a) palladium(II) acetate; (b) palladium(II) acetylacetonate and (c) palladium(II) chloride. (d) Sample XPS spectrum for the mechanochemically prepared NP-lignin composite from the PdCl₂ precursor.

5 Whereas all samples demonstrated the presence of PdNPs, the samples generated from PdCl₂ largely consisted of NPs clearly located outside of the lignin matrix. In contrast, both the acetate and the acetylacetonate precursors yielded composites in which the PdNPs were distributed throughout the organic matrix. The choice of the precursor only marginally affected the size of the resulting NPs, with average sizes
 10 measured to be 3.2, 2.8 and 3.6 nm with PdCl₂, Pd(acetate)₂ and Pd(acac)₂ respectively. The NPs size dispersity and shape were also dependent on the precursor. The NPs formed from PdCl₂ outside of the organic matrix exhibited a diversity of shapes and a standard deviation of 1.6 nm. An improved monodispersity was observed for particles obtained from Pd(acetate)₂ and Pd(acac)₂ with values of
 15 0.7 and 0.9 respectively. The obtained particles were also more spherical in shape. In all cases, XPS analysis revealed that the NPs consist of Pd⁰ and Pd^{II}O species²⁷ and FTIR-ATR confirmed the oxidation of the lignin structure and thus its reducing role in the process (See ESI).²⁸ These results reveal a clear correlation between the size and shape control of the resulting PdNPs and the ability for the system to
 20 properly embed them inside the lignin matrix. It is also likely that lignin here acts not only as a reducer, but also as a stabilizer, since its presence in high concentration at the PdNP surface affords better control over the growth process. We hypothesize

that the difference between the chloride-based and the metal-organic precursors resides in their compatibility with the organic matrix. The metal-organic precursors demonstrate a clear superiority to incorporate within the non-polar lignin structure.

Preparation of RuNP@lignin composites

5 Attempts to synthesize lignin composites containing embedded RuNPs revealed similar behaviour to Pd-based systems. The synthesis of the composites was explored using two commercially and readily accessible metal precursors, the inorganic, ionic ruthenium(III) chloride hydrate ($\text{RuCl}_3 \cdot n\text{H}_2\text{O}$) and the trinuclear μ -oxo metal-organic complex, basic Ru(III) acetate. Both precursors produced NPs
 10 upon milling with Kraft lignin. However, samples prepared using RuCl_3 did not exhibit any NPs under TEM analysis of the washed sample, despite the oxidation of lignin evidenced by FTIR-ATR (ESI). Next, we analysed the washings of this reaction product by TEM and indeed detected RuNPs of $6.7 \pm 4.2\text{nm}$ diameter besides the organic matter composed presumably of nano- and micron-sized lignin
 15 fragments (ESI). On the other hand, the metal-organic complex precursor yielded lignin samples with RuNPs distributed throughout the volume of the organic matrix (Figure 5a,b). As previously, oxidation of lignin was confirmed by FTIR-ATR (ESI).



20 Figure 5. TEM images of RuNPs obtained by milling of Kraft lignin with: (a) basic ruthenium(III) acetate and (b) hydrated ruthenium(III) chloride. XPS spectra of the RuNPs generated by grinding Kraft lignin with: (c) basic ruthenium(III) acetate and (d) hydrated ruthenium(III) chloride.

In both instances the Ru3d XPS spectra of mechanochemical products were identical, exhibiting 3d emission lines consistent with the presence of Ru^{II}O (Figure 5c,d).²⁹ The appearance of RuO is not surprising, as the formation of an oxide layer on ruthenium NPs was previously observed and established to become increasingly prominent with the reduction in particle size.²⁹ Similar to the results obtained with the Pd series, RuNPs produced by mechanochemical synthesis in the presence of lignin have a very different morphology depending on the nature of the Ru precursor. Basic Ru(III) acetate, an organometallic precursor, could easily mix within the lignin upon milling and afforded well embedded RuNPs@lignin composites, while the chloro-metallic species affords RuNPs besides the matrix. Interestingly, the fact that lignin appears oxidized in all cases shows that lignin does reduce Ru precursors even when their uptake within the lignin matrix is negligible. The versatility of this synthetic method is exemplified by the possibility to access either free NPs or matrix supported NPs, by a careful choice of precursor, while using the same bio-based reducer: lignin.

Mechanochemical reduction of rhenium(I) precursors

We have also performed preliminary experiments in generating Re-based nanoparticles through mechanochemical lignin-induced reduction. Milling of Re(CO)₅Br with Kraft lignin for 90 minutes at 29.5 Hz led to the formation of ReNPs, as demonstrated by TEM analysis (Figure 6). The use of Re(CO)₅Br as a metal precursor is particularly interesting due to the presence of a non-ionic halide covalently bound to the metal centre as well as the presence of organometallic CO ligands. The generated ReNPs were found to be highly monodisperse in size with a diameter of 6.2 ± 1.5 nm and distributed neither fully inside the matrix, nor detached from it. The TEM images clearly reveal the ReNPs lying at the surface of the organic matrix, which adopts a morphology similar to snail eyes. FTIR-ATR confirmed, like in all samples described above, the oxidation of the lignin structure (See ESI). However the XPS analysis did not confirm the reduction of the Re species and showed peaks consistent with ReO₂.

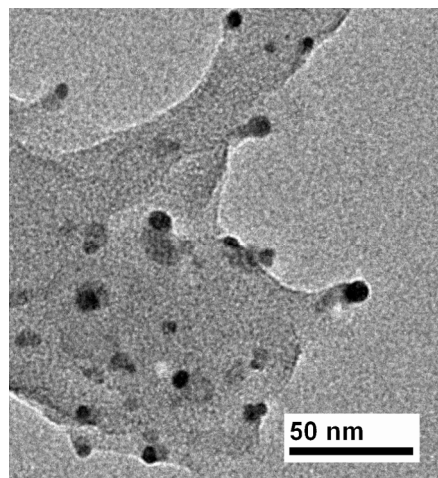


Figure 6. TEM image of the ReNP@lignin composite obtained by mechanical milling of Re(CO)₅Br and lignin.

Conclusion

We have shown, for the first time, the viability of mechanochemical milling with lignin as a means to producing high quality, and highly monodisperse metal NPs. The herein presented mechanochemical methodology was readily applicable to four distinct noble metals: Au, Ru, Pd and Re. In all explored examples lignin was demonstrated to participate as a reducer of metal salts to afford metal NPs which, in some cases, were partially oxidized. An interesting variability of the product structure was observed in dependence on the nature of the metal precursor used. For Pd and Ru, metal chloride precursors afforded metal NPs detached from the lignin matrix, while the use of metal-organic precursors yielded a metal NP@lignin composite. This observation opens up the possibility to use mechanochemical lignin-based reduction procedure to prepare either free or lignin-supported NPs using essentially the same methodology, simply by selecting the right precursor. We perceive the presented study, based on four different metals, as a robust proof-of-concept for a potentially general methodology to synthesize metal nanoparticles. In addition to the generality, which is currently being explored in our laboratory, this methodology also offers several attractive advantages over conventional solution-based NP syntheses, such as reducing the amount of waste, eliminating the use of solvent during synthesis, and enabling the use of an inexpensive reducing agent generated from biomass.

Acknowledgments

We thank the Natural Science and Engineering Research Council of Canada (NSERC) Discovery Grant program, the Canada Foundation for Innovation (CFI), the Canada Research Chairs (CRC), the Fonds de Recherche du Québec – Nature et Technologies (FRQNT) Nouveau Chercheur and Equipe programs, the Centre for Green Chemistry and Catalysis (CGCC), NSERC-Collaborative Research and Training Experience (CREATE) in Green Chemistry and McGill University for their financial support.

References

- ^a Centre for Green Chemistry and Catalysis, Department of Chemistry McGill University, 801 Sherbrooke St. W., H3A 0B8 Montreal, Canada. Tel: +1(514)398 3959; Fax +1(514)398 3797; E-mail: audrey.moores@mcgill.ca; tomlav.friscic@mcgill.ca
- † Electronic Supplementary Information (ESI) available: Experimental Details, TEM Measurements, FTIR-ATR, XPS and PXRD Data. See DOI: 10.1039/b000000x/
1. P. Balaz, M. Achimovicova, M. Balaz, P. Billik, Z. Cherkezova-Zheleva, J. M. Criado, F. Delogu, E. Dutkova, E. Gaffet, F. J. Gotor, R. Kumar, I. Mitov, T. Rojac, M. Senna, A. Streletskii and K. Wiczorek-Ciurova, *Chem. Soc. Rev.*, 2013, **42**, 7571-7637.
 2. C. Suryanarayana, *Progress in Materials Science*, 2001, **46**, 1-184.
 3. V. Sepelak, A. Duvel, M. Wilkening, K.-D. Becker and P. Heitjans, *Chem. Soc. Rev.*, 2013, **42**, 7507-7520.
 4. V. Sepelak, S. Begin-Colin and G. Le Caer, *Dalton Trans.*, 2012, **41**, 11927-11948.
 5. V. Sepelak, I. Bergmann, S. Indris, A. Feldhoff, H. Hahn, K. D. Becker, C. P. Grey and P. Heitjans, *J. Mater. Chem.*, 2011, **21**, 8332-8337.
 6. L. Russo, F. Colangelo, R. Cioffi, I. Rea and L. D. Stefano, *Materials*, 2011, **4**, 1023-1033.
 7. M. J. Rak, N. K. Saade, T. Friscic and A. Moores, *Green Chem.*, 2014, **16**, 86-89.
 8. P. Baláž, M. Baláž, M. Čaplovičová, A. Zorkovska, L. Čaplovič and M. Psoška, *Faraday Discuss.*, 2014.

9. P. Baláz, E. Boldizárová, E. Godočiková and J. Briančin, *Mater. Lett.*, 2003, **57**, 1585-1589.
10. P. Baláz and E. Dutková, *J. Therm. Anal. Calorim.*, 2007, **90**, 85-92.
11. M. Ojeda, A. M. Balu, V. Barron, A. Pineda, A. G. Coletto, A. A. Romero and R. Luque, *J. Mater. Chem. A*, 2014, **2**, 387-393.
- 5 12. A. Pineda, A. M. Balu, J. M. Campelo, R. Luque, A. A. Romero and J. C. Serrano-Ruiz, *Catal. Today*, 2012, **187**, 65-69.
13. J. A. Dahl, B. L. S. Maddux and J. E. Hutchison, *Chem. Rev.*, 2007, **107**, 2228-2269.
14. C. J. Murphy, *J. Mater. Chem.*, 2008, **18**, 2173-2176.
- 10 15. A. K. Mohanty, M. Misra and L. T. Drzal, *J. Polym. Environ.*, 2002, **10**, 19-26.
16. P. Anastas and N. Eghbali, *Chem. Soc. Rev.*, 2010, **39**, 301-312.
17. D. Stewart, *Industrial Crops and Products*, 2008, **27**, 202-207.
18. T. Kleine, J. Buendia and C. Bolm, *Green Chem.*, 2013, **15**, 160-166.
19. Z.-H. Wu, D.-Y. Lee, M. Matsuoka and M. Sumimoto, *Mokuzai Gakkaishi*, 1991, **37**, 164-171.
- 15 20. Z.-H. Wu and M. Sumimoto, *Mokuzai Gakkaishi*, 1992, **38**, 277-284.
21. J. Virkutyte and R. S. Varma, *Chemical Science*, 2011, **2**, 837-846.
22. W. Thielemans, E. Can, S. S. Morye and R. P. Wool, *J. Appl. Polym. Sci.*, 2002, **83**, 323-331.
- 20 23. M. Lucas, B. A. Macdonald, G. L. Wagner, S. A. Joyce and K. D. Rector, *ACS Appl. Mater. Interfaces*, 2010, **2**, 2198-2205.
24. F. Coccia, L. Tonucci, D. Bosco, M. Bressan and N. d'Alessandro, *Green Chem.*, 2012, **14**, 1073-1078.
25. N. H. Turner and A. M. Single, *Surf. Interface Anal.*, 1990, **15**, 215-222.
- 25 26. C.-H. Wang, C.-C. Chien, Y.-L. Yu, C.-J. Liu, C.-F. Lee, C.-H. Chen, Y. Hwu, C.-S. Yang, J.-H. Je and G. Margaritondo, *J. Synchrotron. Radiat.*, 2007, **14**, 477-482.
27. M. Brun, A. Berthet and J. C. Bertolini, *J. Electron Spectrosc. Relat. Phenom.*, 1999, **104**, 55-60.
28. T. Schalow, B. Brandt, D. E. Starr, M. Laurin, S. K. Shaikhutdinov, S. Schauer mann, J. Libuda and H.-J. Freund, *Angew. Chem., Int. Ed.*, 2006, **45**, 3693-3697.
- 30 29. M. E. Grass, Y. Zhang, D. R. Butcher, J. Y. Park, Y. Li, H. Bluhm, K. M. Bratlie, T. Zhang and G. A. Somorjai, *Angew. Chem., Int. Ed.*, 2008, **47**, 8893-8896.

35 *****